**Table A1.** Geographic information (latitude, longitude, elevation above sea level) for CASTNet sites used in our analysis. Sites determined to be regionally-representative are indicated in **bold**.

| Region | Site ID | Station Name | State | Latitude (° N) | Longitude (° W) | Elevation (m ASL) |
|---|---|---|---|---|---|---|
| Northwest | **NCS** | **North Cascades NP** | **WA** | **48.5** | **121.4** | **109** |
| | OLY | Olympic NP | WA | 48.1 | 123.4 | 125 |
| | **MOR** | **Mount Rainier NP** | **WA** | **46.8** | **122.1** | **421** |
| | GLR | Glacier NP | MT | 48.5 | 114.0 | 976 |
| California | LAV | Lassen Volcanic NP | CA | 40.5 | 121.6 | 1756 |
| | **DEV** | **Death Valley NM** | **CA** | **36.5** | **116.8** | **125** |
| | PIN | Pinnacles NM | CA | 36.5 | 121.2 | 335 |
| | JOT | Joshua Tree NM | CA | 34.1 | 116.4 | 1244 |
| | **YOS** | **Yosemite NP - Turtleback Dome** | **CA** | **37.7** | **119.7** | **1605** |
| Mountain West | CNT | Centennial | WY | 41.4 | 106.2 | 3178 |
| | GTH | Gothic | CO | 39.0 | 107.0 | 2926 |
| | GRB | Great Basin NP | NV | 39.0 | 114.2 | 2060 |
| | **MEV** | **Mesa Verde NP** | **CO** | **37.2** | **108.5** | **2165** |
| | **PND** | **Pinedale** | **WY** | **42.9** | **109.8** | **2388** |
| | ROM | Rocky Mountain NP | CO | 40.3 | 105.5 | 2743 |
| | YEL | Yellowstone NP | WY | 44.6 | 110.4 | 2469 |
| | **GRC** | **Grand Canyon NP** | **AZ** | **36.1** | **112.2** | **2073** |
| | CAN | Canyonlands NP | UT | 38.5 | 109.8 | 1814 |
| | CHA | Chiricahua NM | AZ | 32.0 | 109.4 | 1570 |
| Plains | **CAD** | **Caddo Valley** | **AR** | **34.2** | **93.1** | **71** |
| | **STK** | **Stockton** | **IL** | **42.3** | **90.0** | **274** |
| | VOY | Voyageurs NP | MN | 48.4 | 92.8 | 427 |
| | ALH | Alhambra | IL | 38.9 | 89.6 | 164 |
| | **BVL** | **Bondville** | **IL** | **40.1** | **88.4** | **212** |
| | PRK | Perkinstown | WI | 45.2 | 90.6 | 472 |
| | VIN | Vincennes | IN | 38.7 | 87.5 | 134 |
| Great Lakes | ANA | Ann Arbor | MI | 42.4 | 83.9 | 267 |
| | HOX | Hoxeyville | MI | 44.2 | 85.7 | 305 |
| | UVL | Unionville | MI | 43.6 | 83.4 | 201 |
| | **SAL** | **Salamonie Reservoir** | **IN** | **40.8** | **85.7** | **250** |
| | **DCP** | **Deer Creek** | **OH** | **39.6** | **83.3** | **267** |
| | LYK | Lykens | OH | 40.9 | 83.0 | 303 |
| | **OXF** | **Oxford** | **OH** | **39.5** | **84.7** | **284** |
| | QAK | Quaker City | OH | 39.9 | 81.3 | 372 |
| | KEF | Kane Exp. Forest | PA | 41.6 | 78.8 | 622 |
| | LRL | Laurel Hill | PA | 40.0 | 79.3 | 615 |
| | **MKG** | **M.K. Goddard** | **PA** | **41.4** | **80.1** | **384** |
| | CDR | Cedar Creek | WV | 38.9 | 80.8 | 234 |
| | PAR | Parsons | WV | 39.1 | 79.7 | 510 |
| Northeast | **WSP** | **Washington Crossing** | **NJ** | **40.3** | **74.9** | **61** |
| | ARE | Arendtsville | PA | 39.9 | 77.3 | 269 |
| | **PSU** | **Penn State** | **PA** | **40.7** | **77.9** | **378** |
| | **CTH** | **Connecticut Hill** | **NY** | **42.4** | **76.7** | **501** |
| | ABT | Abington | CT | 41.8 | 72.0 | 209 |
| Far Northeast | WST | Woodstock | NH | 43.9 | 71.7 | 258 |
| | ACA | Acadia NP | ME | 44.4 | 68.3 | 152 |
| | **ASH** | **Ashland** | **ME** | **46.6** | **68.4** | **235** |
| | **HOW** | **Howland** | **ME** | **45.2** | **68.7** | **69** |
| Southeast | BEL | Beltsville | MD | 39.0 | 76.8 | 46 |
| | BWR | Blackwater NWR | MD | 38.4 | 76.1 | 4 |
| | VPI | Horton Station | VA | 37.3 | 80.6 | 920 |
| | PED | Prince Edward | VA | 37.2 | 78.3 | 150 |
| | SHN | Shenandoah NP - Big Meadows | VA | 38.5 | 78.4 | 1073 |
| | **CDZ** | **Cadiz** | **KY** | **36.8** | **87.8** | **189** |
| | CKT | Crockett | KY | 37.9 | 83.1 | 455 |
| | MCK | Mackville | KY | 37.7 | 85.0 | 353 |
| | ESP | Edgar Evins | TN | 36.0 | 85.7 | 302 |
| | GRS | Great Smoky NP - Look Rock | TN | 35.6 | 83.9 | 793 |
| | **SPD** | **Speedwell** | **TN** | **36.5** | **83.8** | **361** |
| | COW | Coweeta | NC | 35.1 | 83.4 | 686 |
| | PNF | Cranberry | NC | 36.1 | 82.0 | 1219 |
| | BFT | Beaufort | NC | 34.9 | 76.6 | 2 |
| | **CND** | **Candor** | **NC** | **35.3** | **79.8** | **198** |
| | **SND** | **Sand Mountain** | **AL** | **34.3** | **86.0** | **352** |
| | CVL | Coffeeville | MS | 34.0 | 89.8 | 134 |
| | GAS | Georgia Station | GA | 33.2 | 84.4 | 270 |
| Florida / Gulf | **EVE** | **Everglades NP** | **FL** | **25.4** | **80.7** | **2** |
| | **SUM** | **Sumatra** | **FL** | **30.1** | **85.0** | **14** |

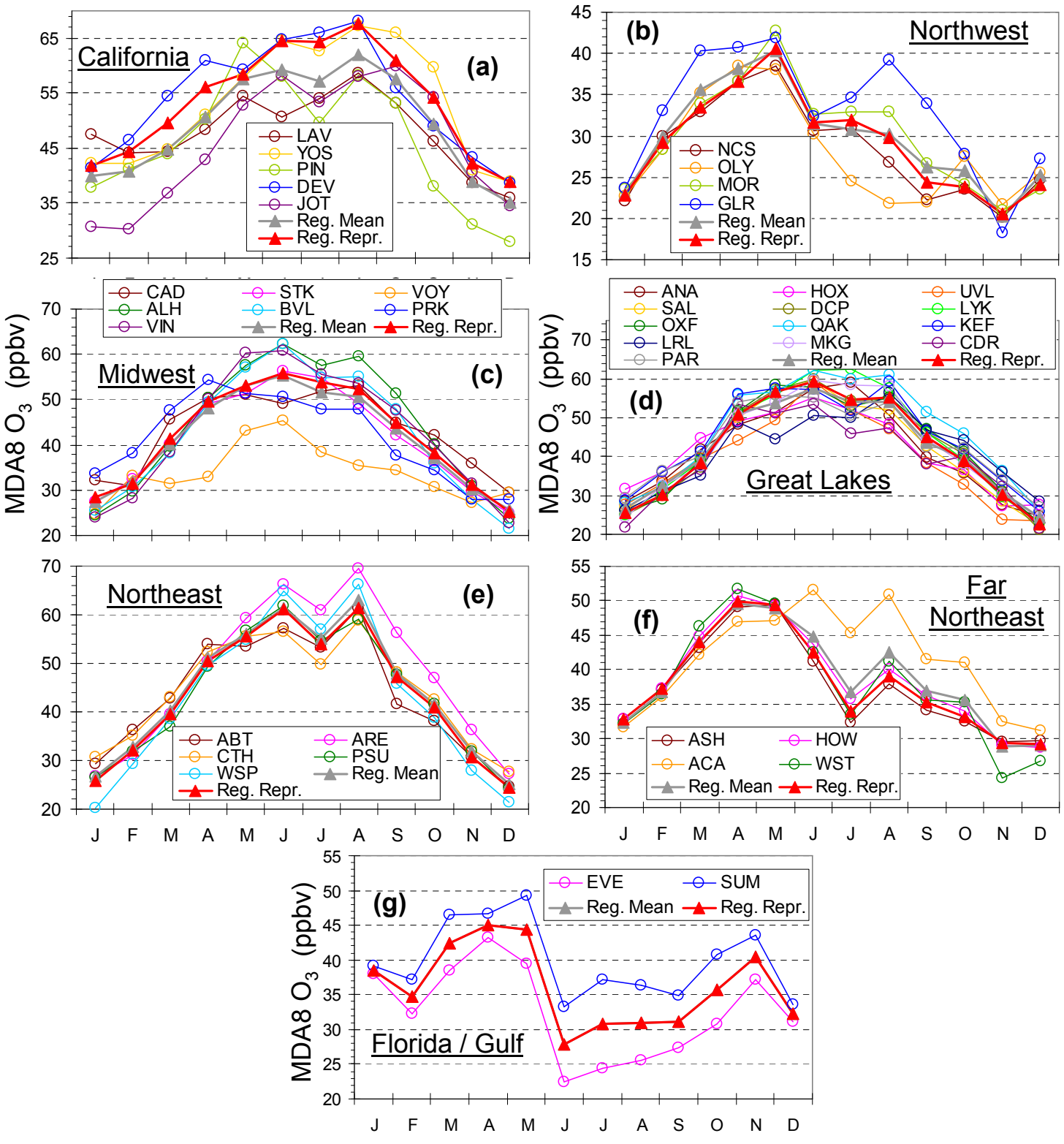


**Figure A1.** As in Fig. 2, but for the other seven regions. The regionally-representative sites (mean shown as solid red triangles) are: Northwest - MOR, NCS; California - DEV, YOS; Plains - BVL, CAD, STK; Great Lakes - DCP, MKG, OXF, SAL; Northeast - CTH, PSU, WSP; Far Northeast - ASH, HOW; Florida / Gulf - EVE, SUM. Note the range of magnitudes on the y-axes.

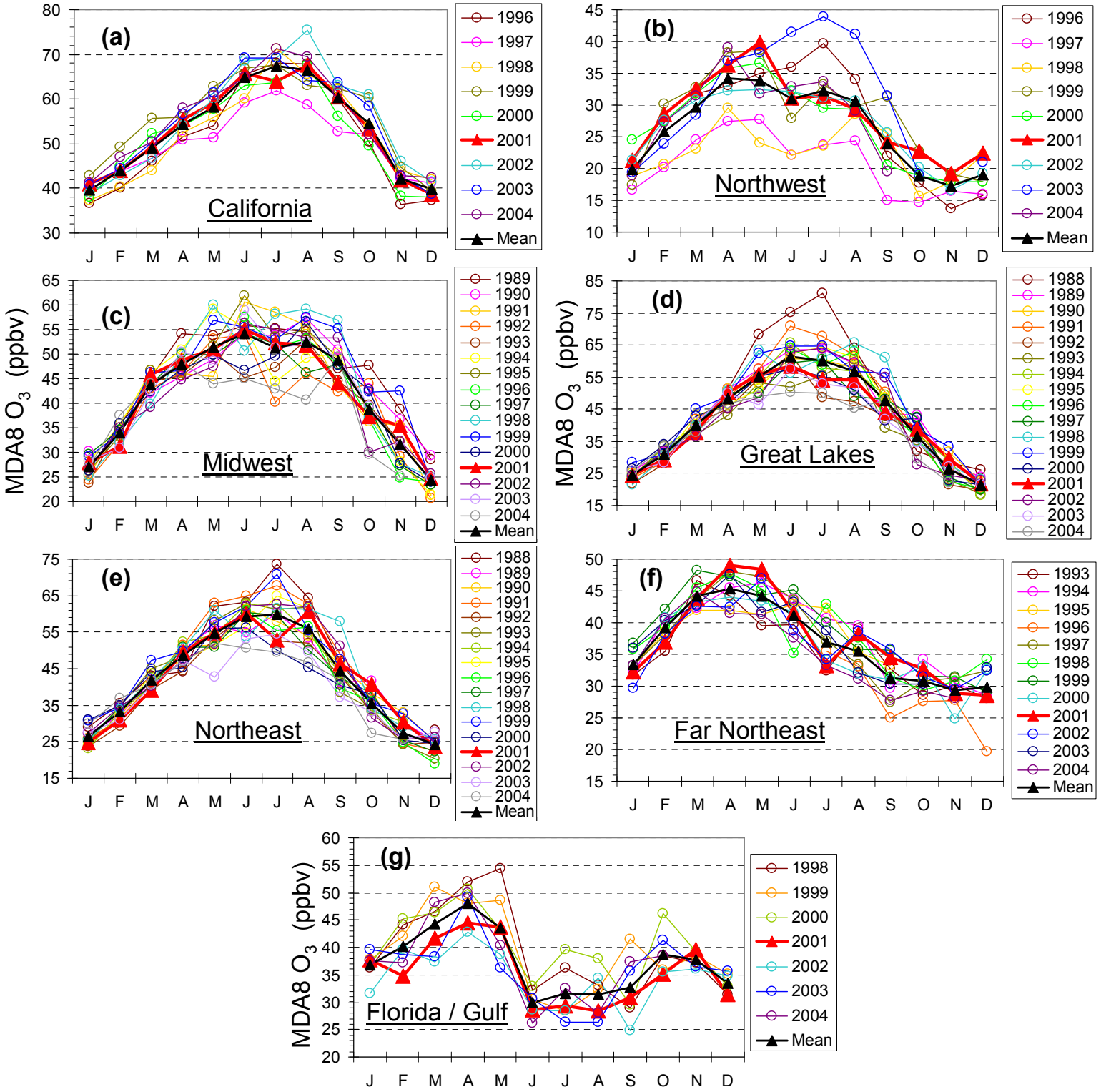


**Figure A2.** As in Fig. 3, but for the other seven regions.

**Table A2.** Details of the global models used in our analysis, including emissions inventories and meteorological fields employed for the HTAP simulations. Further description of model characteristics is available at: http://www.mi.uni-hamburg.de/List-classification-and-detail-view-of-model-entr.567.0.html. Adapted from *Fiore et al.* [2009].

| Model | Resolution (lon x lat x layers) | Institution | Model contact | Anthropogenic emission inventory for $O_3$ precursors | Driving meteorology (year 2001) |
|---|---|---|---|---|---|
| CAMCHEM-3311m13# | 2.5° x 2° x 30 | NCAR, USA | Peter Hess | POET for 1997[a]; CO fossil fuel and biofuel from a MOPITT inversion[b] | NCEP |
| ECHAM5-HAMMOZ-v21 | 2.81° x 2.81° x 21 | EPFL, Switzerland | Gerd Folberth | RETRO | ECMWF ERA-40 |
| EMEP-rv26# (NH only) | 1° x 1° x 20 | EMEP, Norway | Jan Eiof Jonson, Peter Wind | IER / Uni-Stuttgart, based on EDGAR2000; EMEP | ECMWF ERA-40 |
| FRSGC/UCI v01# | 2.81° x 2.81° x 37 | Lancaster University, UK | Oliver Wild | ACCENT/AR4[c] | ECMWF IFS[d] |
| GEMAQ-EC | 2° x 2° x 20 | Environment Canada | Sunling Gong | AURAMS (regional Canadian, US and Mexico); EDGAR elsewhere | Canadian Meteorological Centre (CMC) |
| GEMAQ-v1p0# | 4° x 4° x 28 | York University, Canada | Alexandru Lupu | EDGAR v2 | CMC |
| GEOS-Chem v07# | 2.5° x 2° x 30 | Harvard University, USA | Rokjin Park | Bey et al., 2001[e] | NASA GEOS-4 |
| GEOS-Chem v07-res4x5 | 5° x 4° x 30 | CIEMAT, Spain | Marta Garcia Vivanco | EMEP emissions EPA/NEI99 inventory | NASA GEOS-4 |
| GISS-PUCCNI-modelE# | 5° x 4° x 23 | NASA GISS, USA | Drew Shindell | ACCENT / AR4, with EA emissions of CO and $NO_x$ times 1.66 | NCEP, via linear relaxation |
| GMI-v02f# | 2.5° x 2° x 42 | NASA GSFC, USA | Bryan Duncan | Harvard's merged inventory (NEI99, BRAVO, Streets, EMEP) | NASA GEOS-4 |
| LMDz3-INCA1# | 3.75° x 2.5° x 19 | LSCE, France | Sophie Szopa | RETRO | ECMWF ERA-40 |
| LLNL-IMPACT-T5a# | 2.5° x 2° x 48 | LLNL, USA | Cynthia Atherton, Daniel Bergmann | POET | NASA GEOS-4-ceres |
| MOZART-GFDL-v2# | 1.88° x 1.88° x 28 | GFDL, USA | Arlene Fiore | EDGAR v2 | NCEP |
| MOZECH-v16# | 2.81 x 2.81 x 31 | FZ Jülich, Germany | Martin Schultz, Sabine Schröder | RETRO | ECMWF ERA-40 |
| Oslo CTM2 | 2.81° x 2.81° x 40 | University of Oslo, Norway | Michael Gauss | EDGAR v3.2 | ECMWF - IFS |
| TM5-JRC-cy2-ipcc-v1# | 1° x 1° x 25 | JRC, Italy | Frank Dentener, Elina Marmer | ACCENT / AR4 | ECMWF |

# - Model used in $NO_x$+CO+VOC+aerosol emission perturbation simulations (all 16 used for "base-case" comparisons)

[a] - Granier, C. et al. (2004), Present and future surface emissions of atmospheric compounds, European Commission report EVK 2199900011. (Available at http:// http://www.aero.jussieu.fr/projet/ACCENT/POET.php)

[b] - Pétron, G., C. Granier, B. Khattatov, V. Yudin, J. Lamarque, L. Emmons, J. Gille, and D. P. Edwards (2004), Monthly CO surface sources inventory based on the 2000 - 2001 MOPITT satellite data, *Geophys. Res. Lett.*, 31, L21107, doi:10.1029/2004GL020560.

[c] - Bond, T.C. et al. (2004), A technology-based global inventory of black and organic carbon emissions from combustion, *J. Geophys. Res.*, 109, D14203, doi:10.1029/2003JD003697.

[d] - van der Werf, G.R., J.T. Randerson, L. Giglio, G.J. Collatz, P.S. Kasibhatla, and A.F. Arellano, Jr. (2006), Interannual variability in global biomass burning emissions from1997 to 2004, *Atmos. Chem. Physics*, 6, 3423-3441.

[e] - based on EDGAR v3.2, see *Stevenson et al.* [2006]

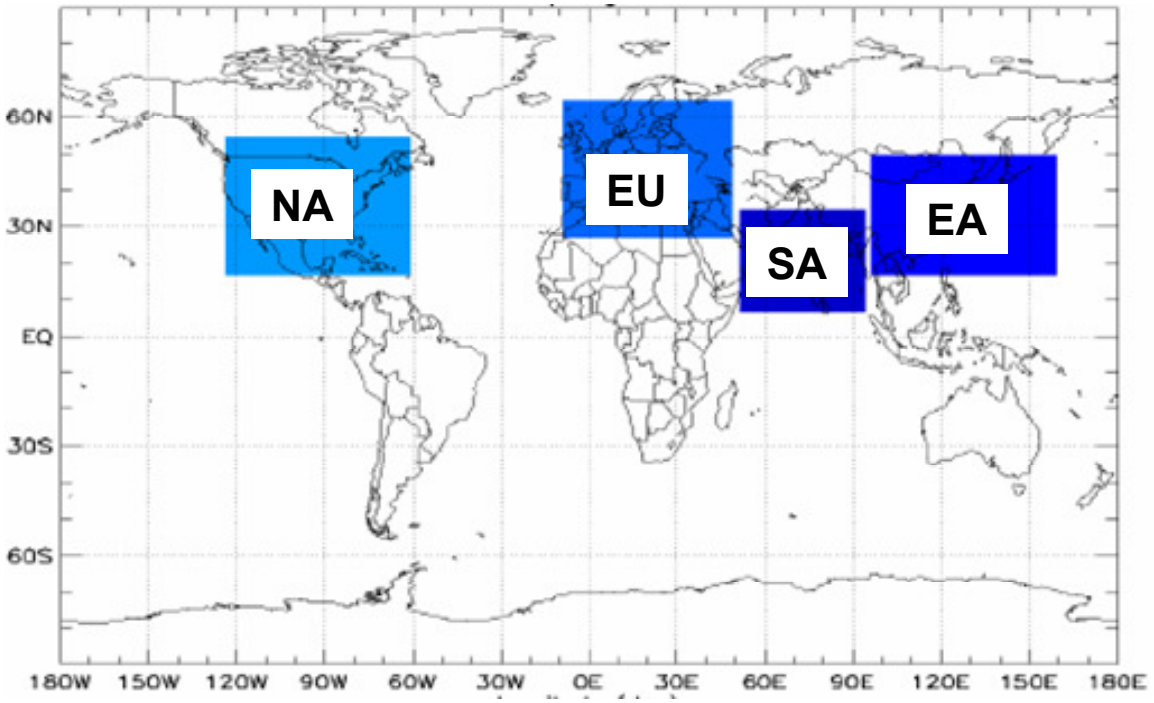


**Figure A3.** Colored boxes represent the four source regions used in the HTAP emissions reductions simulations: NA - North America, EU - Europe, SA - South Asia, EA - East Asia [adapted from *TF HTAP*, 2007].

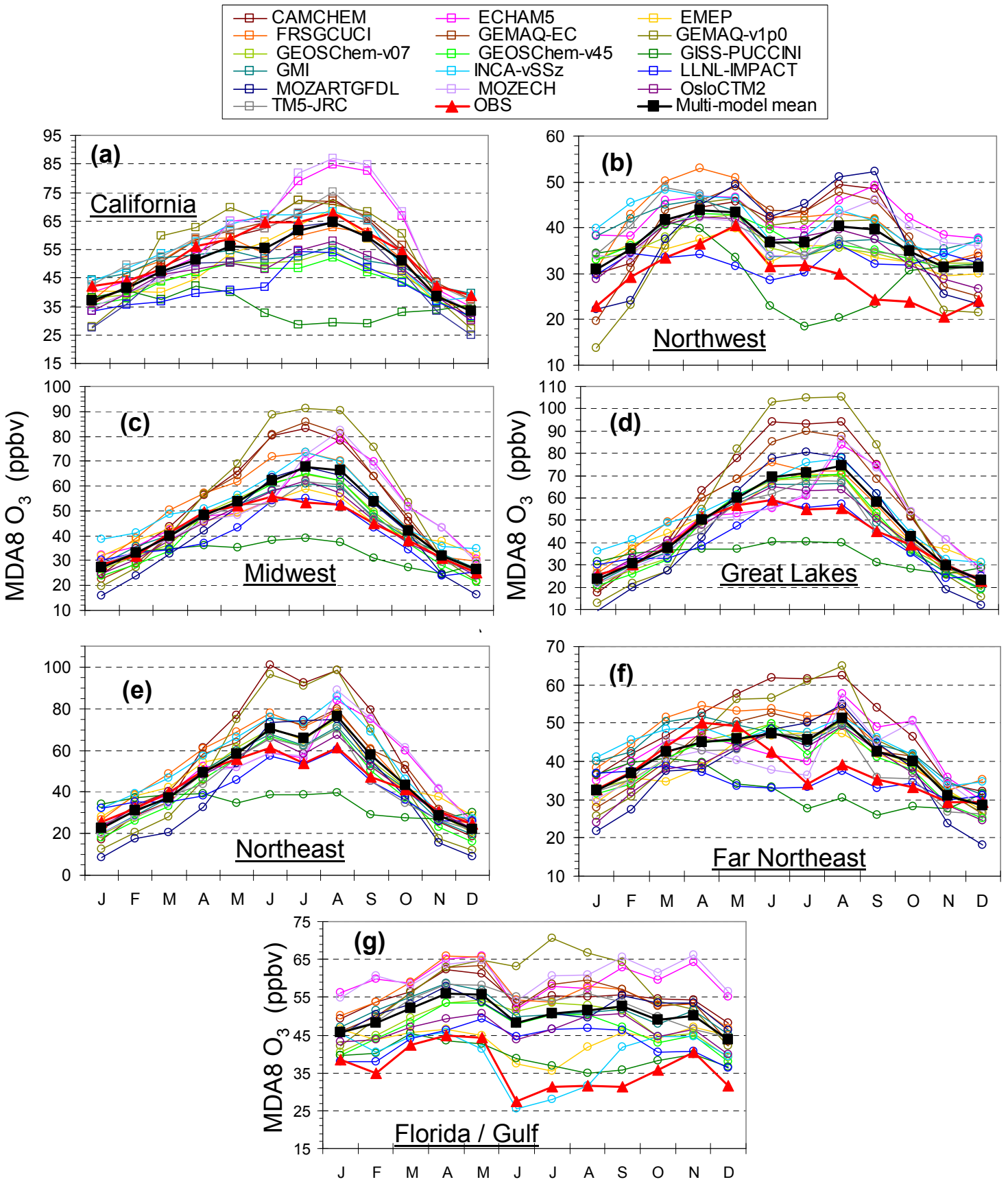


**Figure A4.** Evaluation of multi-model vs.observed values of MBDA $O_3$ for the regions not shown in Fig. 4. Individual models are shown with open circles; multi-model mean as solid black squares and observations as solid red triangles.

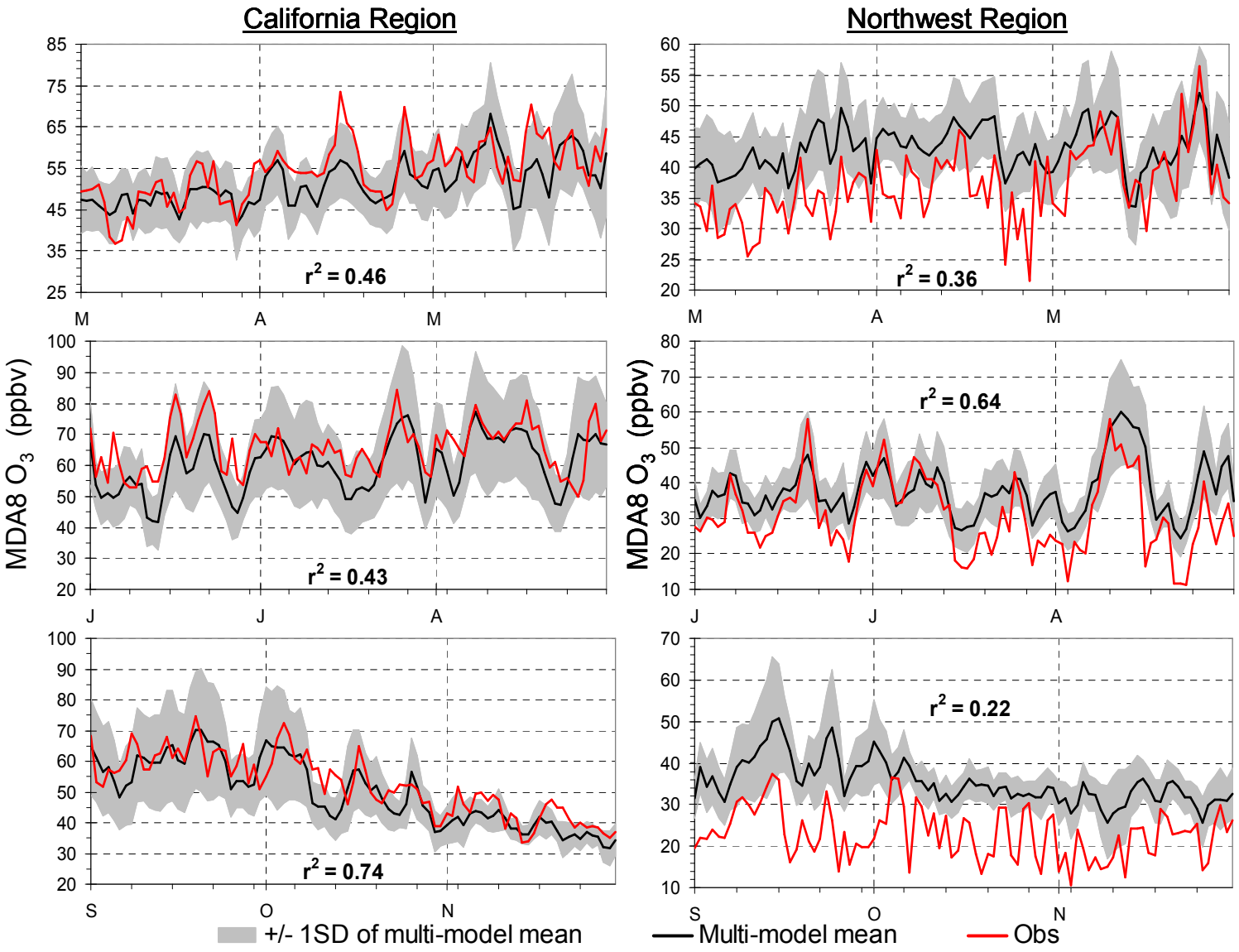


**Figure A5.** Daily MDA8 $O_3$ from observations (red line), multi-model ensemble mean (black line) and 1σ of ensemble mean (gray shading) for spring (MAM), summer (JJA) and autumn (SON) in the seven regions not shown in Fig. 5. Note the range of magnitudes on the y-axes.

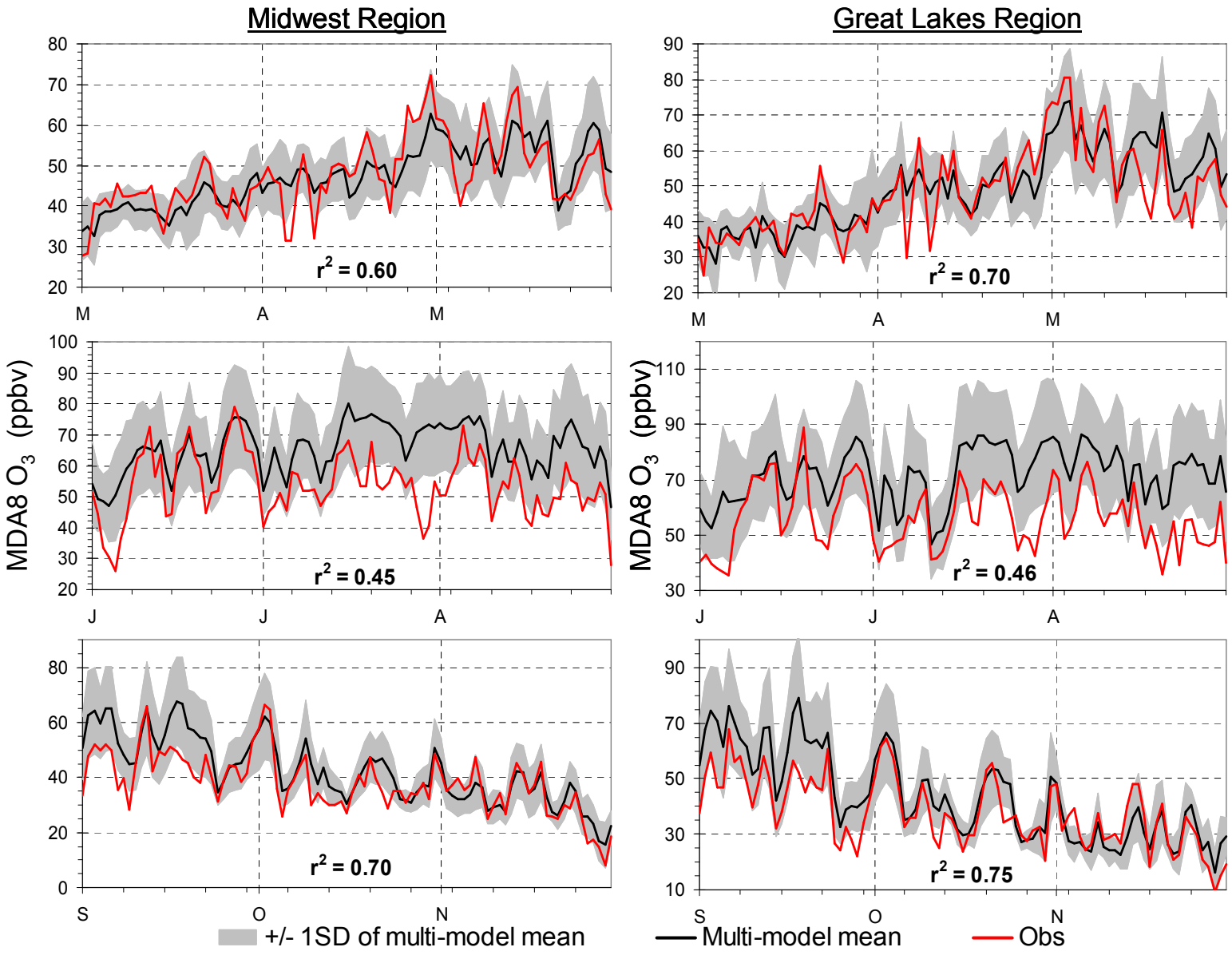


**Figure A5.** (cont'd)

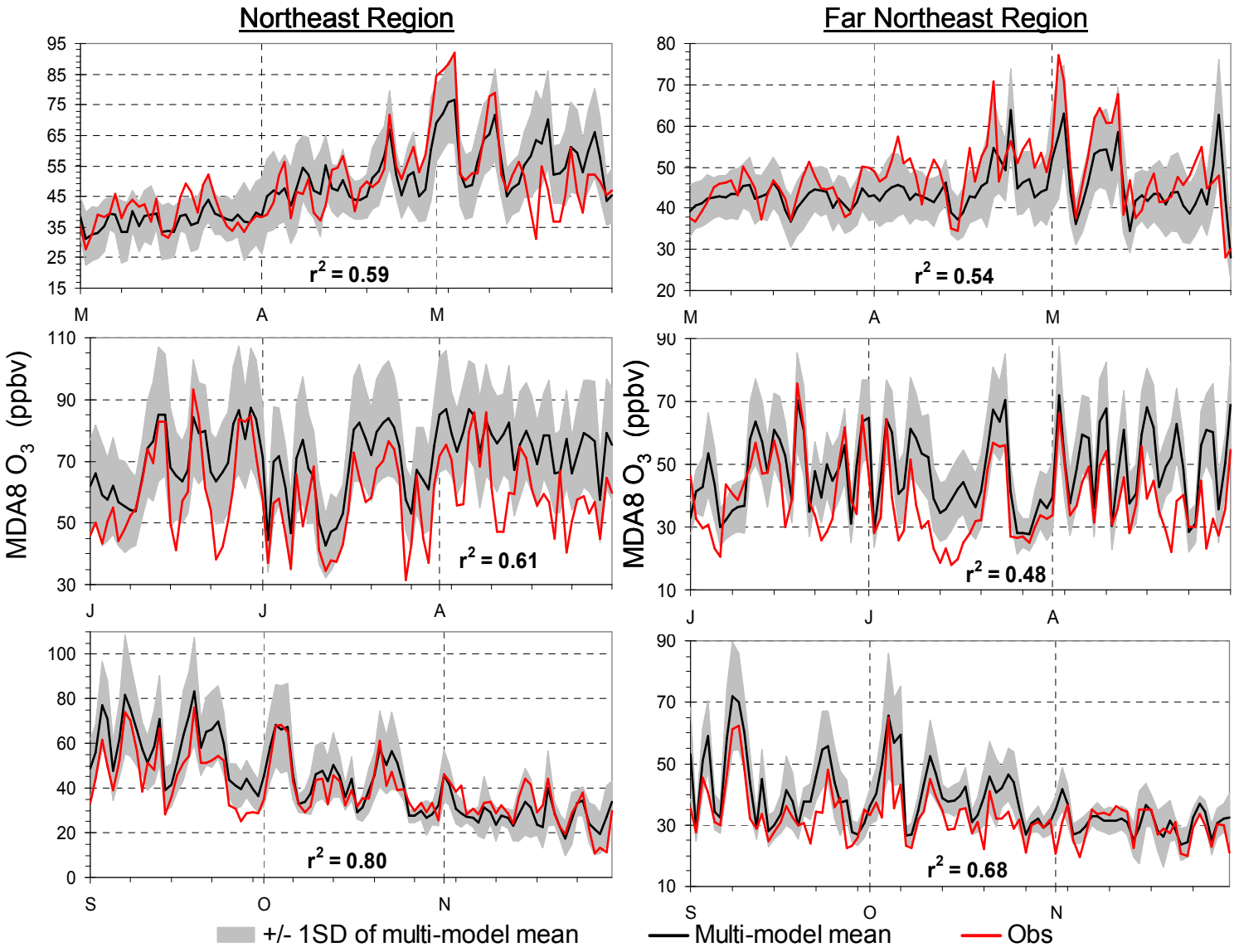


**Figure A5.** (cont'd)

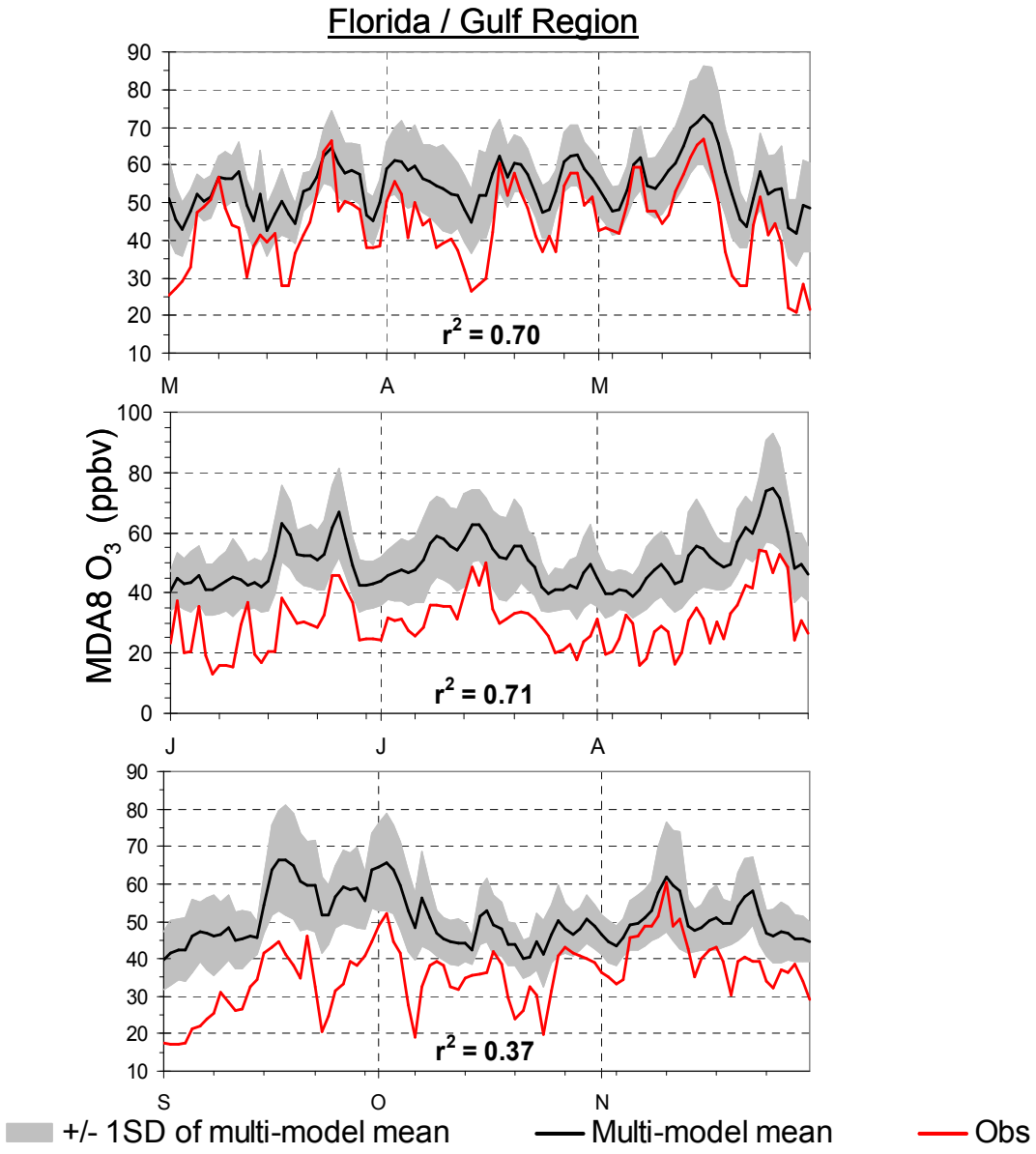


**Figure A5.** (cont'd)

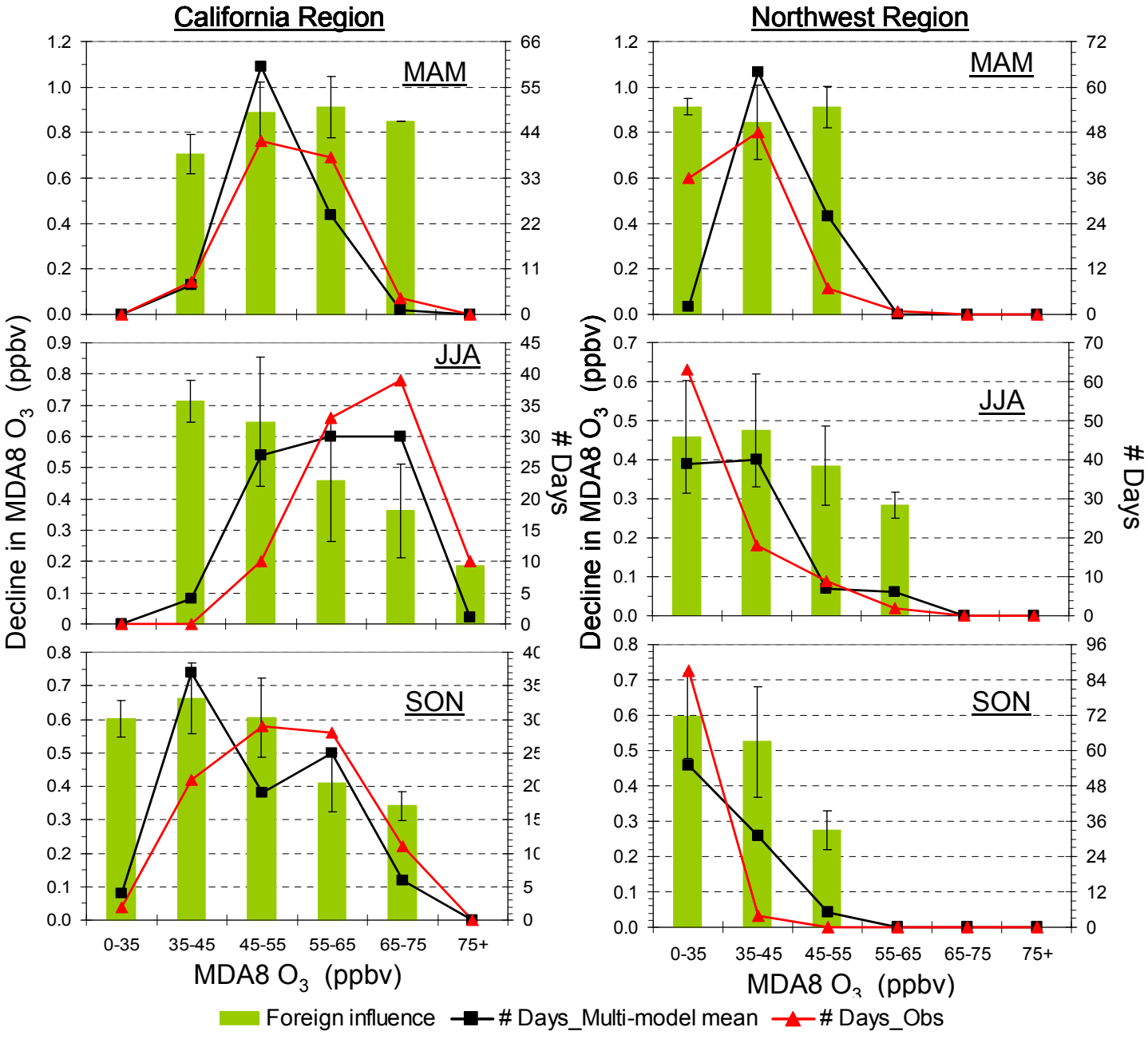


**Figure A6.** Number of days for each MDA8 $O_3$ bin (right-axis) from the multi-model ensemble (black squares) and observations (red triangles) and the sum of the responses of MDA8 $O_3$ to 20% reductions in anthropogenic $O_3$-precursor emissions ($NO_x$ + CO + NMVOC + aerosols) in the three foreign source regions (left-axis; green columns with error bars representing 1σ of the multi-model mean) in the seven regions not shown in Fig. 6, binned by simulated MDA8 $O_3$, for spring (MAM), summer (JJA) and autumn (SON). Note the range of magnitudes on the y-axes.

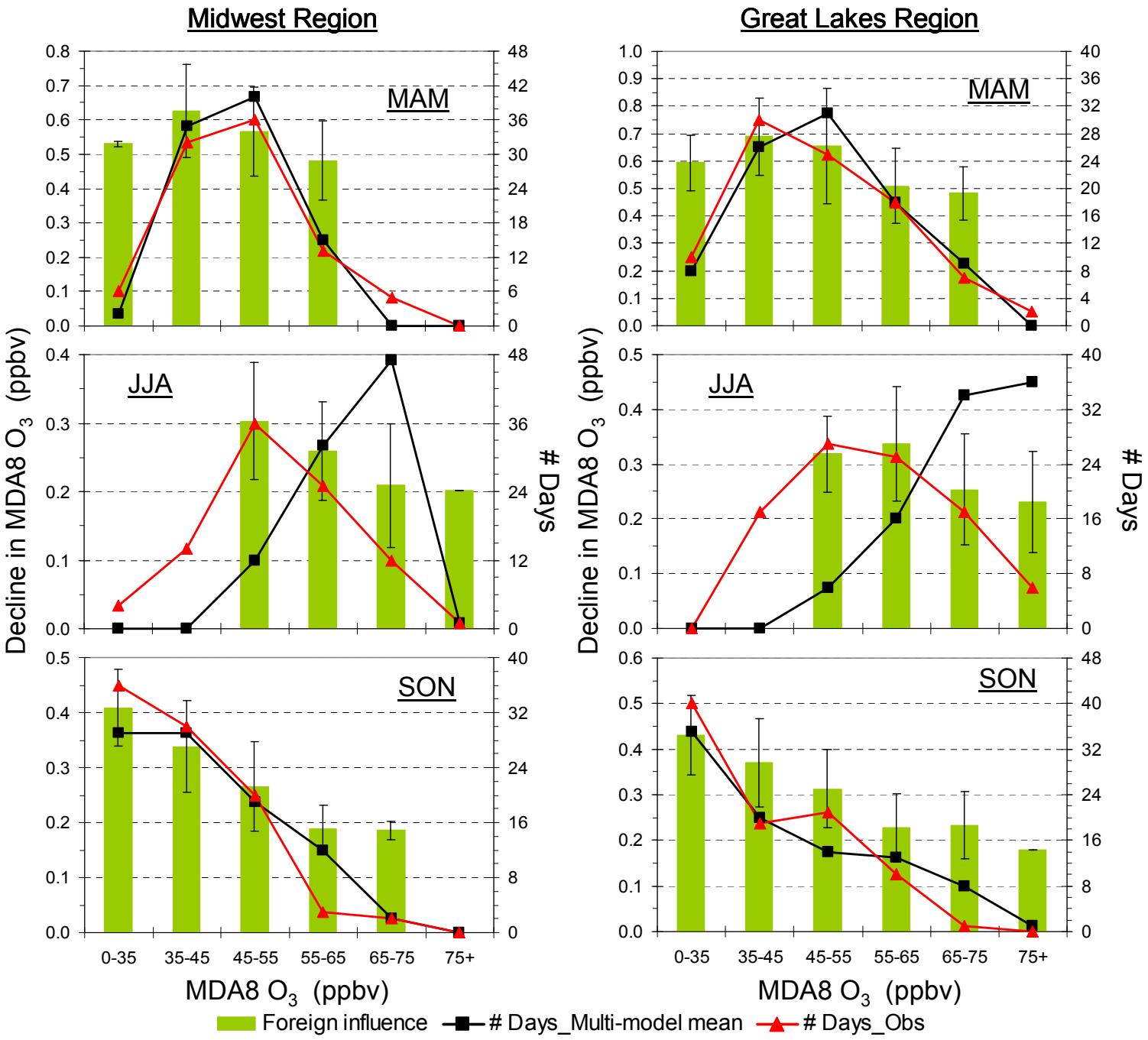


**Figure A6.** (cont'd)

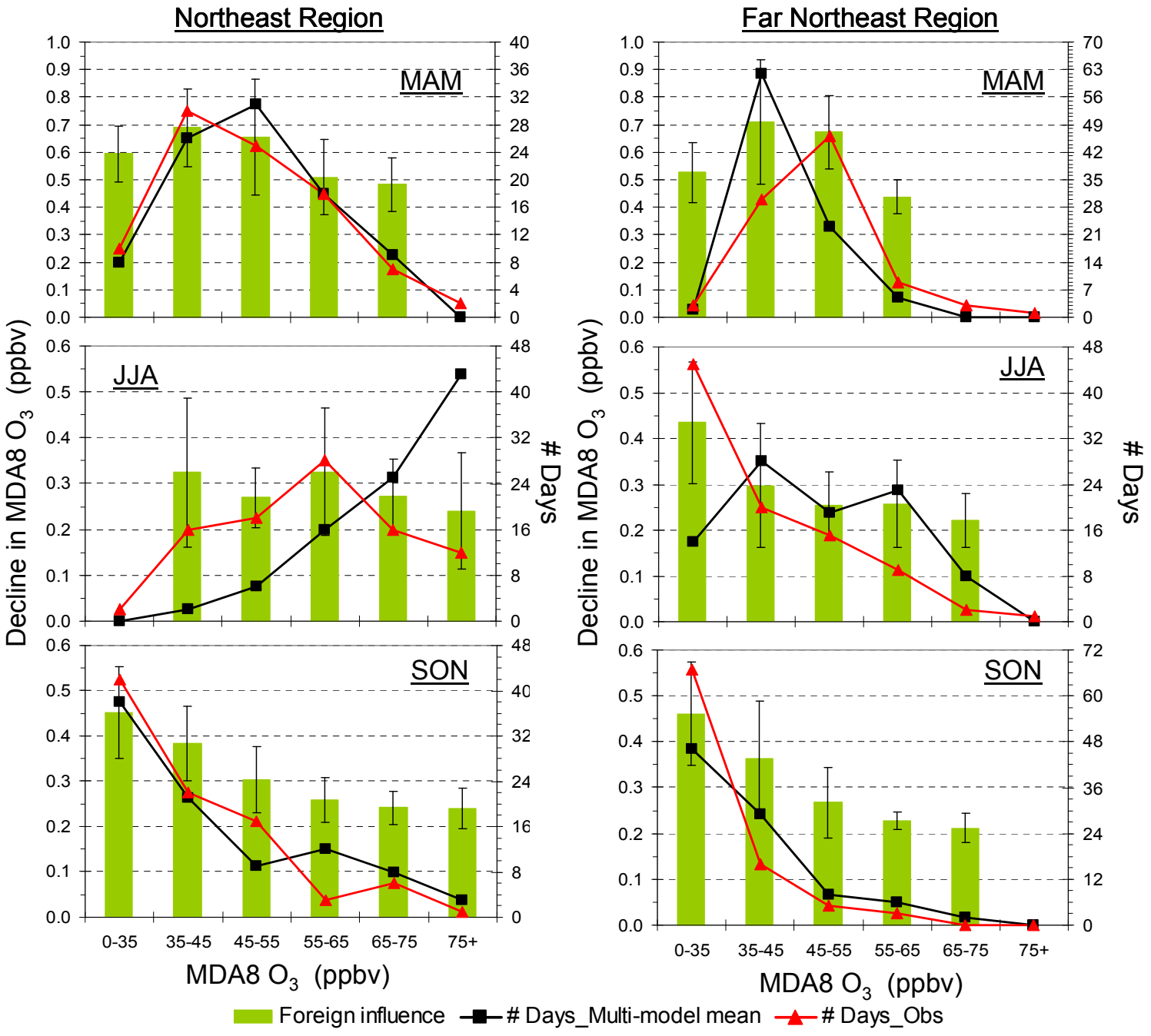


**Figure A6.** (cont'd)

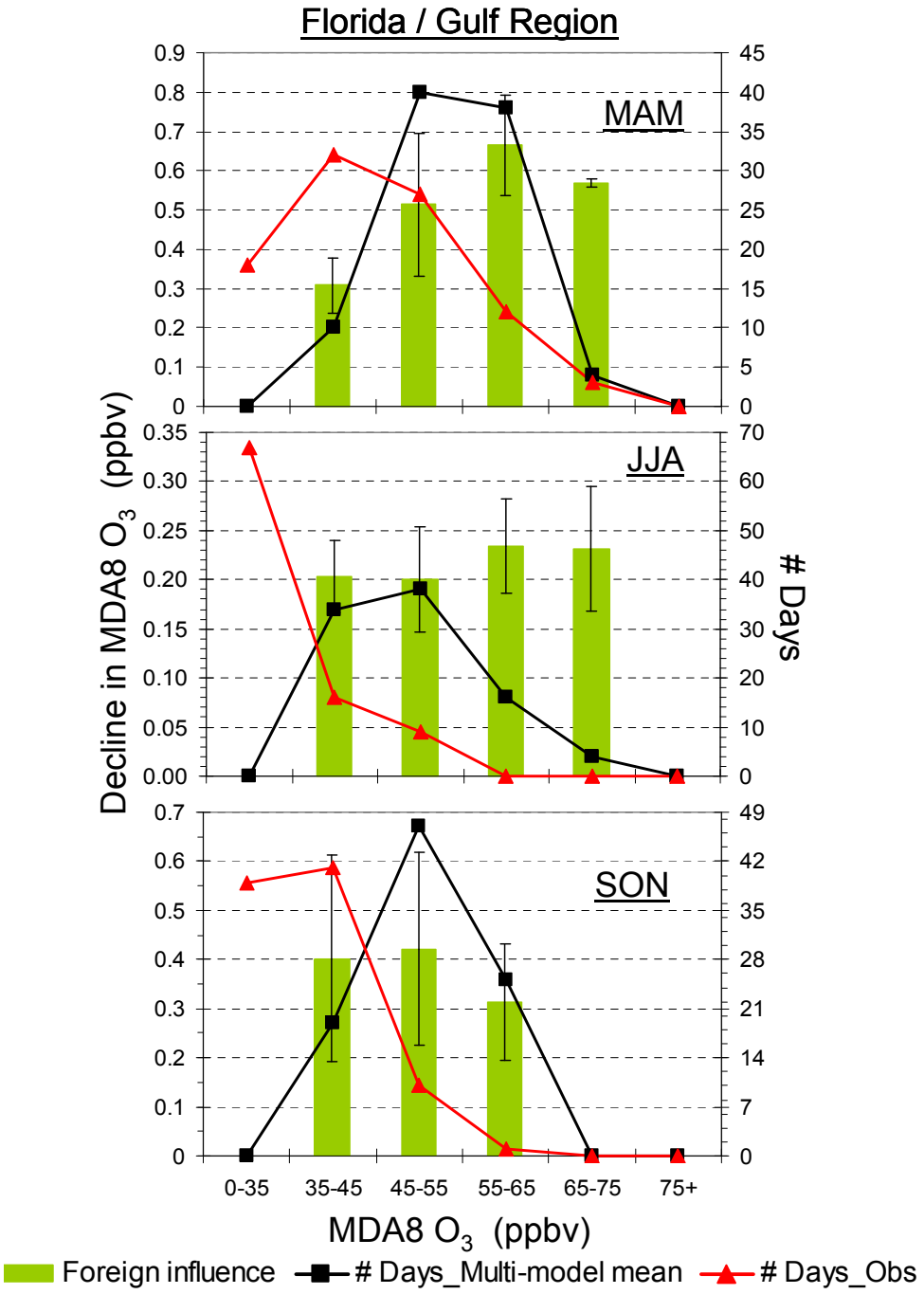


**Figure A6.** (cont'd)

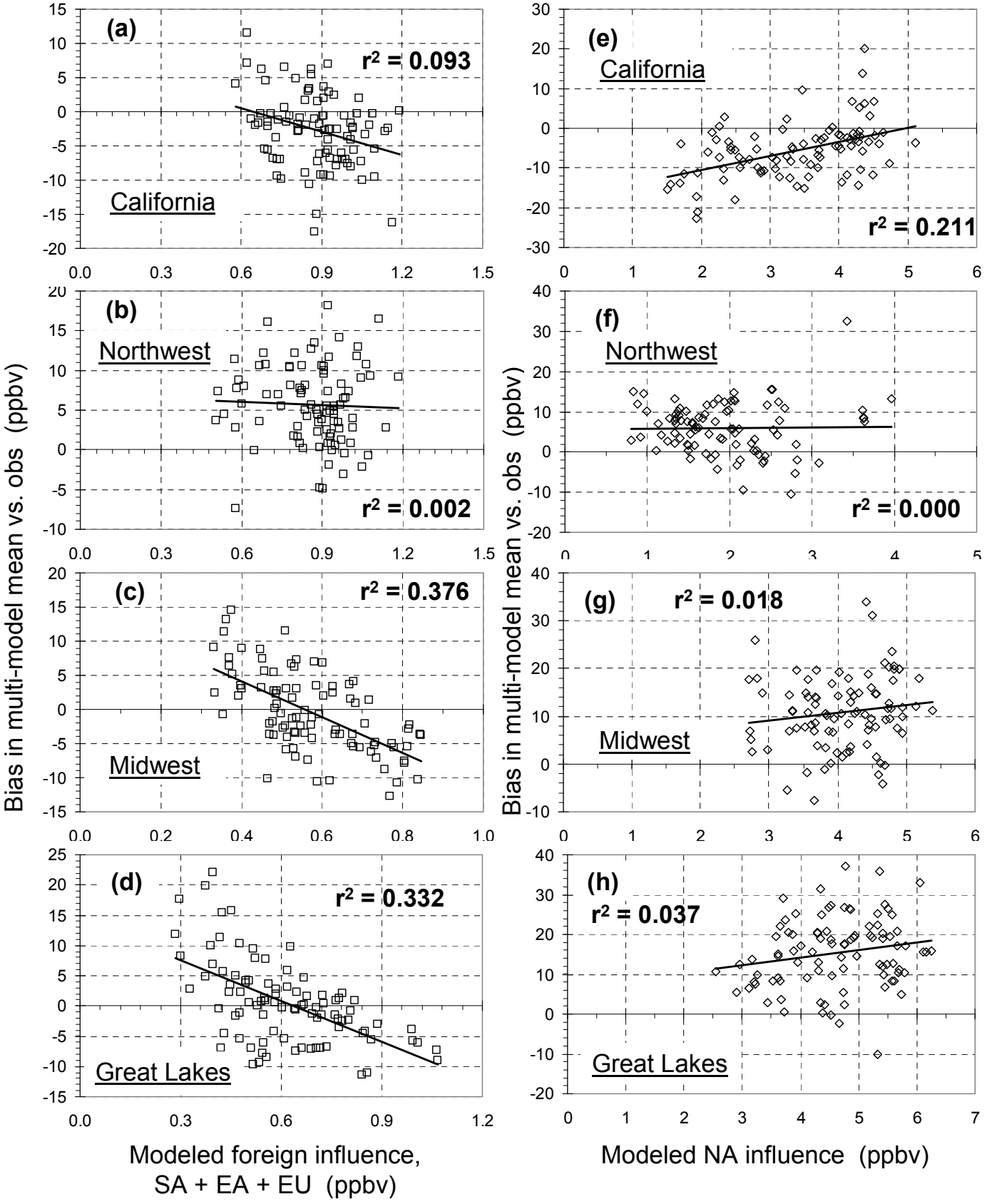


**Figure A7.** As in Fig. 7, but for the other seven regions.

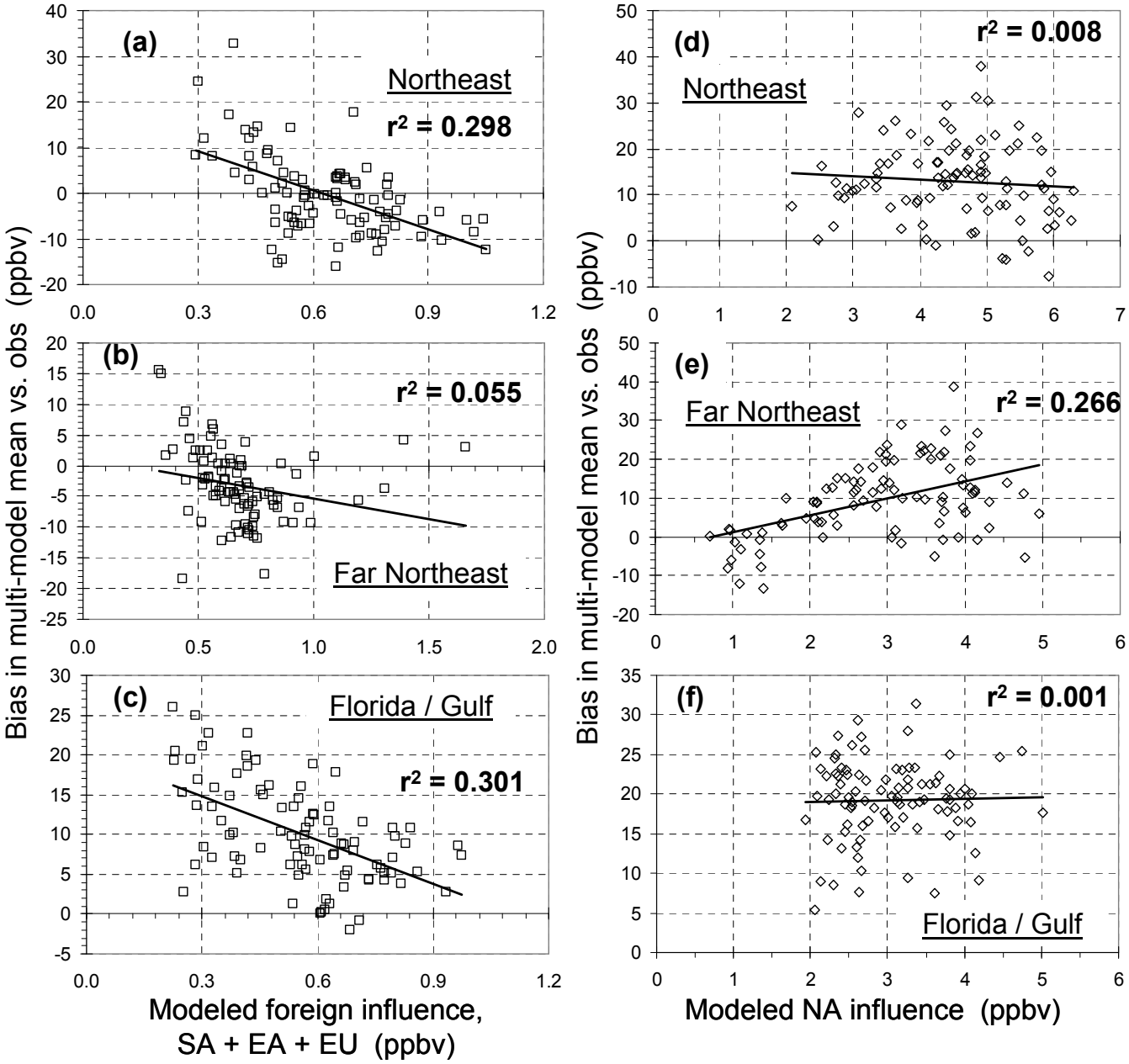


**Figure A7.** (cont'd)

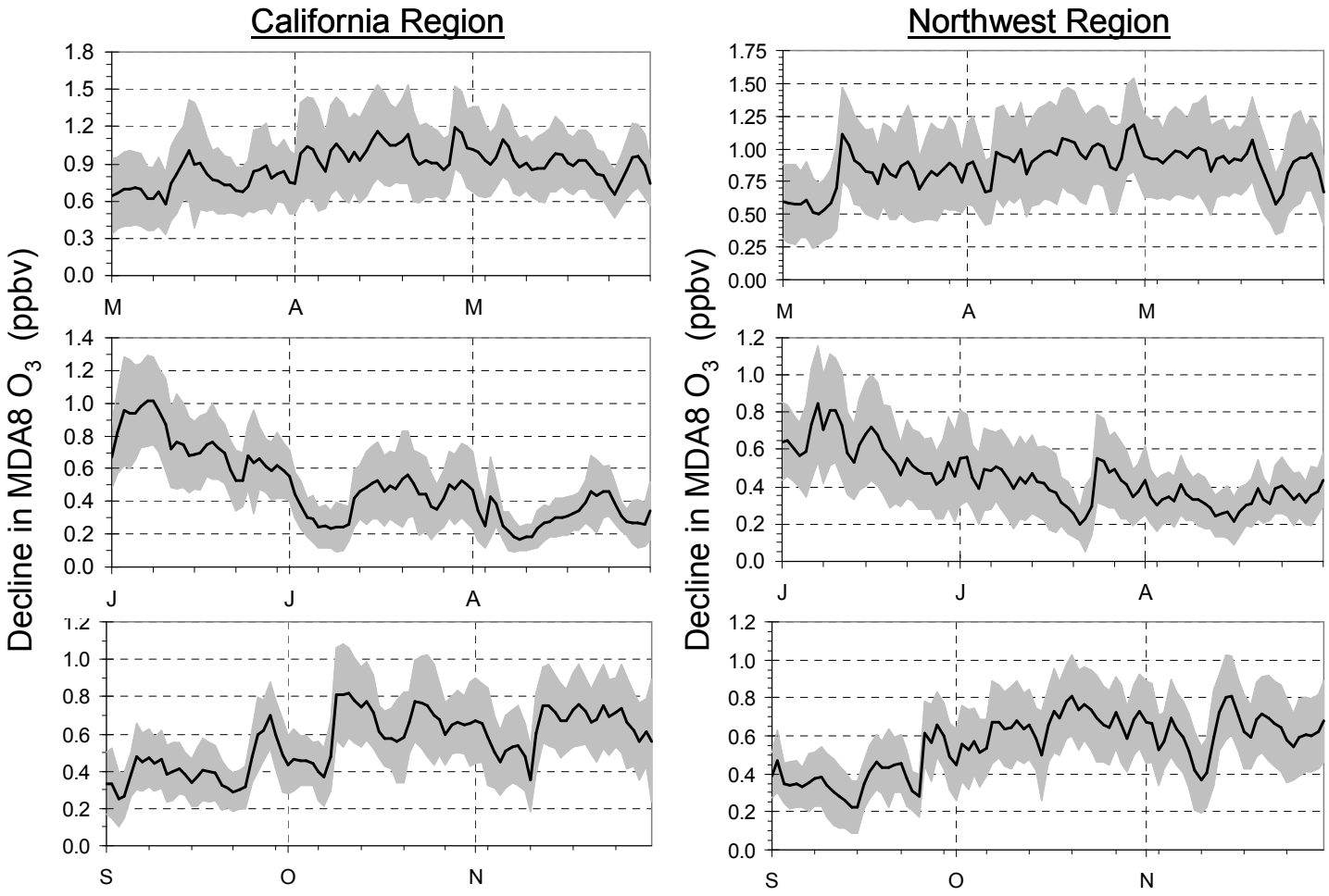


**Figure A8.** Multi-model mean (black line) and 1σ of the ensemble mean (gray shading) in the day-to-day variability of the response of MDA8 $O_3$ to a 20% reduction in anthropogenic $O_3$–precursor emissions ($NO_x$ + CO + NMVOC + aerosols) in the three foreign sources regions (Fig. A3) for the 7 regions not shown in Fig. 8. Note the range of magnitudes on the y-axes.

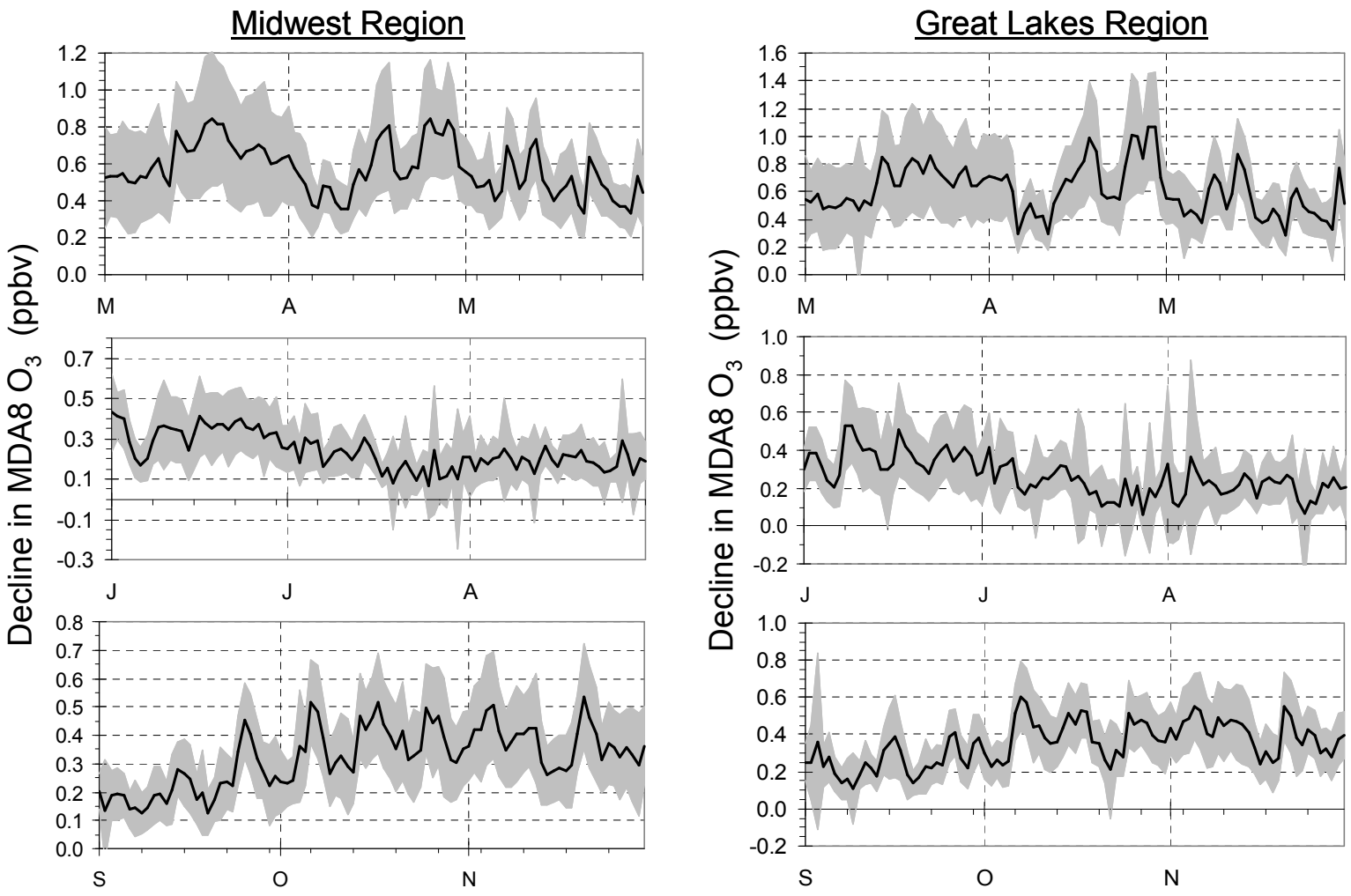


**Figure A8.** (cont'd)

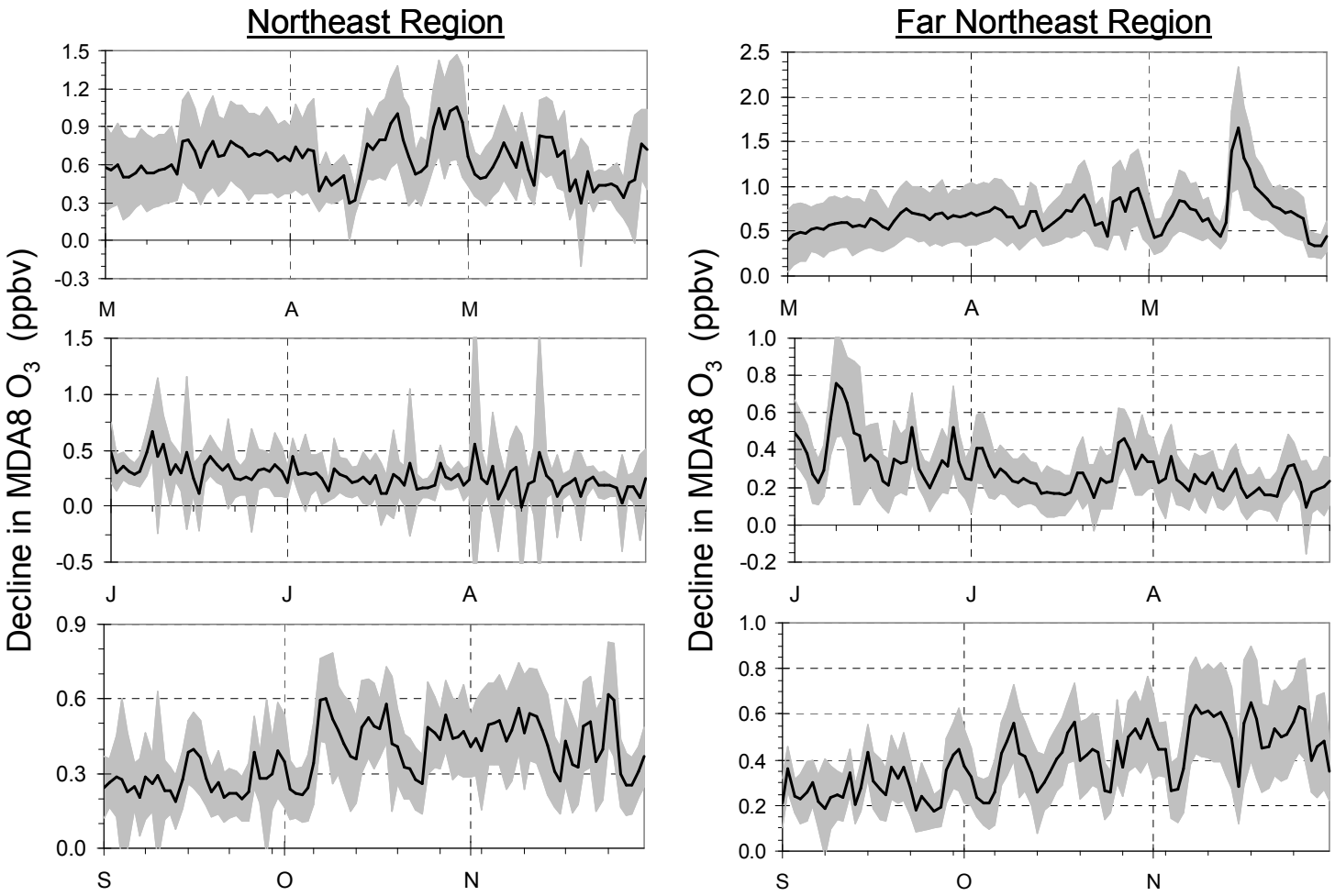


**Figure A8.** (cont'd)

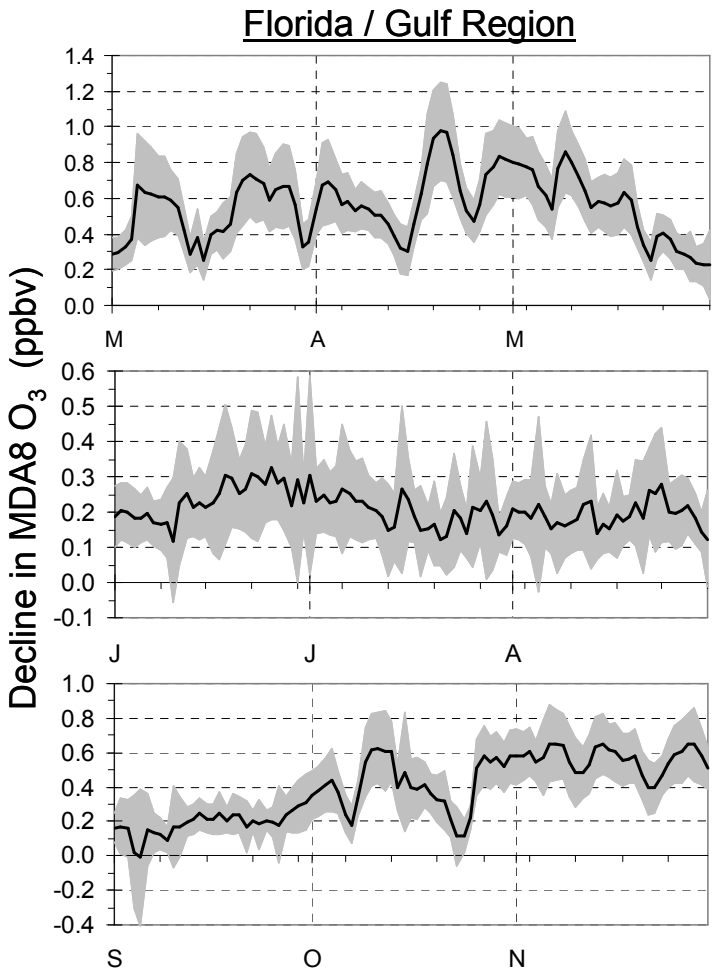


**Figure A8.** (cont'd)

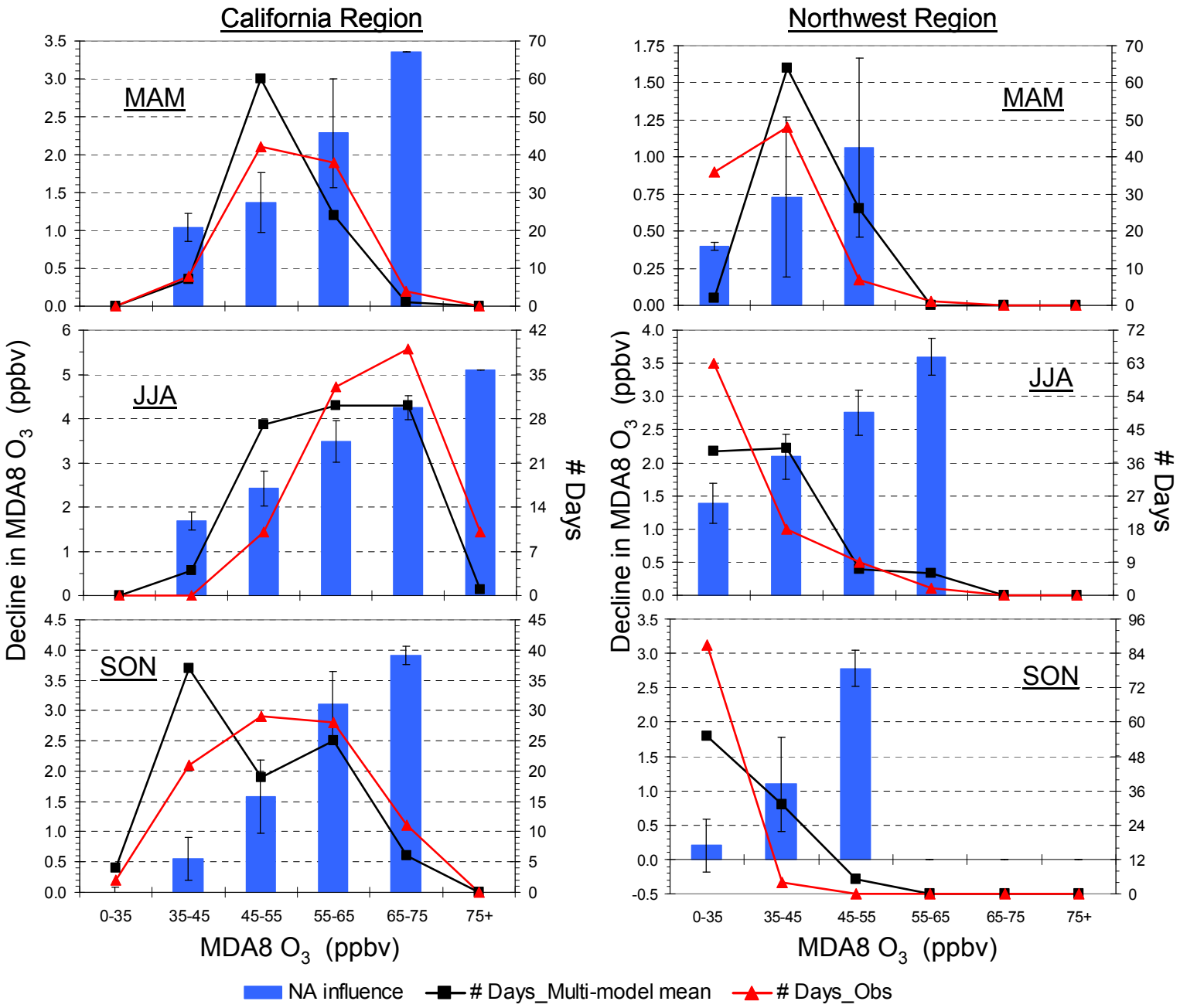


**Figure A9.** As in Fig. A6, but for a 20% emissions reduction of anthropogenic $O_3$-precursors ($NO_x$ + CO + NMVOC + aerosols) in the North American source region (shown in Fig. A3). Note the range of magnitudes on the y-axes.

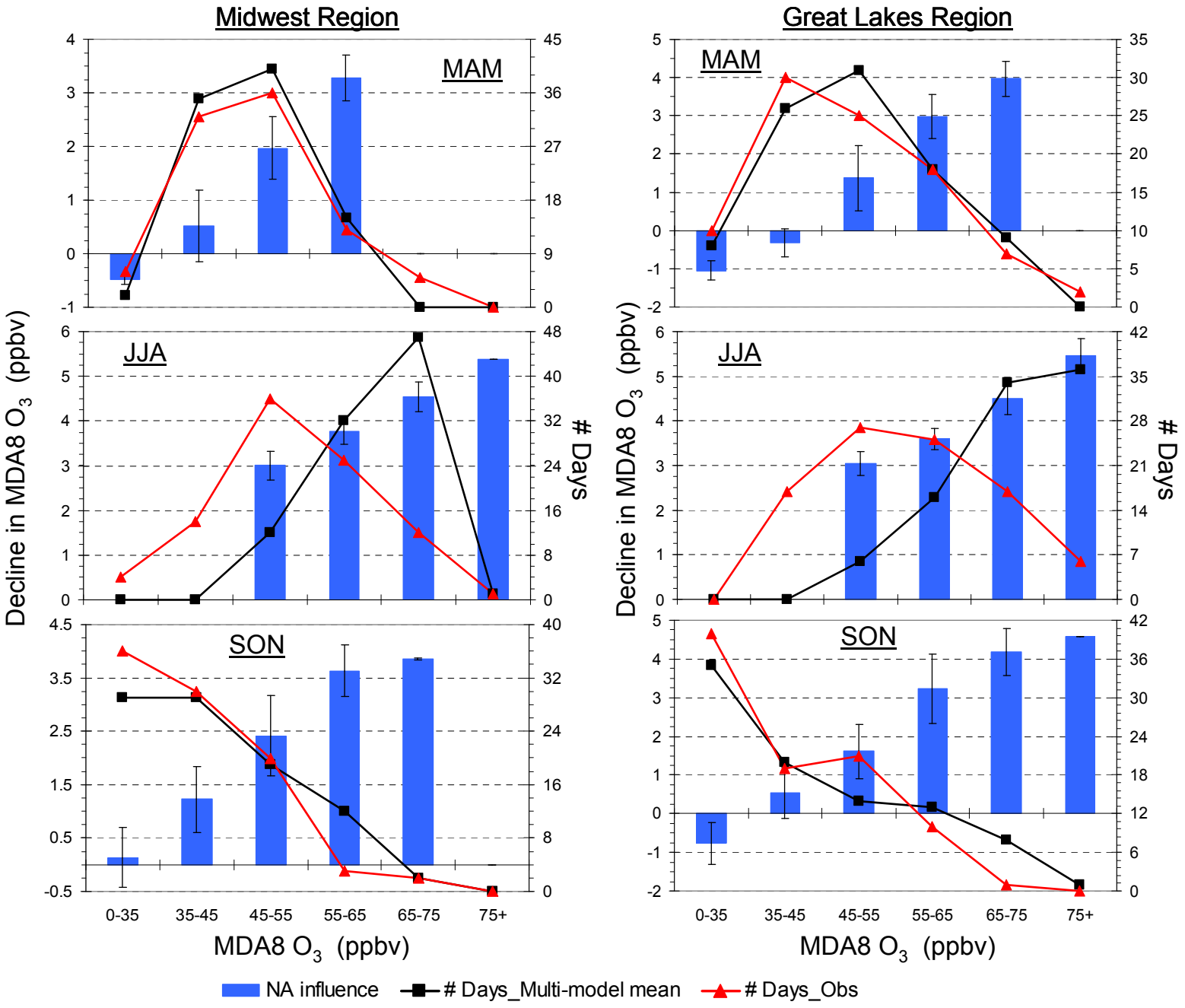


**Figure A9.** (cont'd)

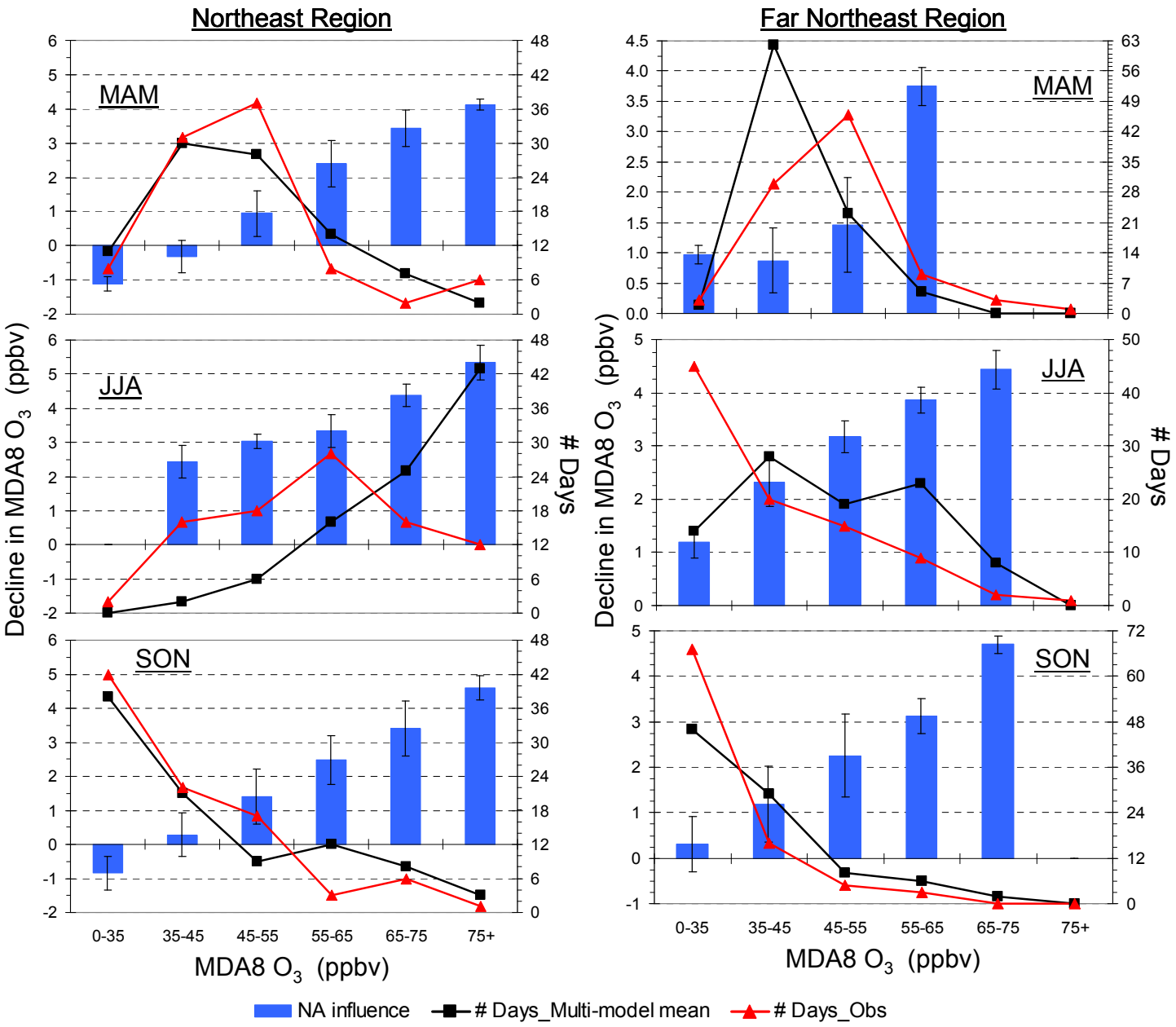


**Figure A9.** (cont'd)

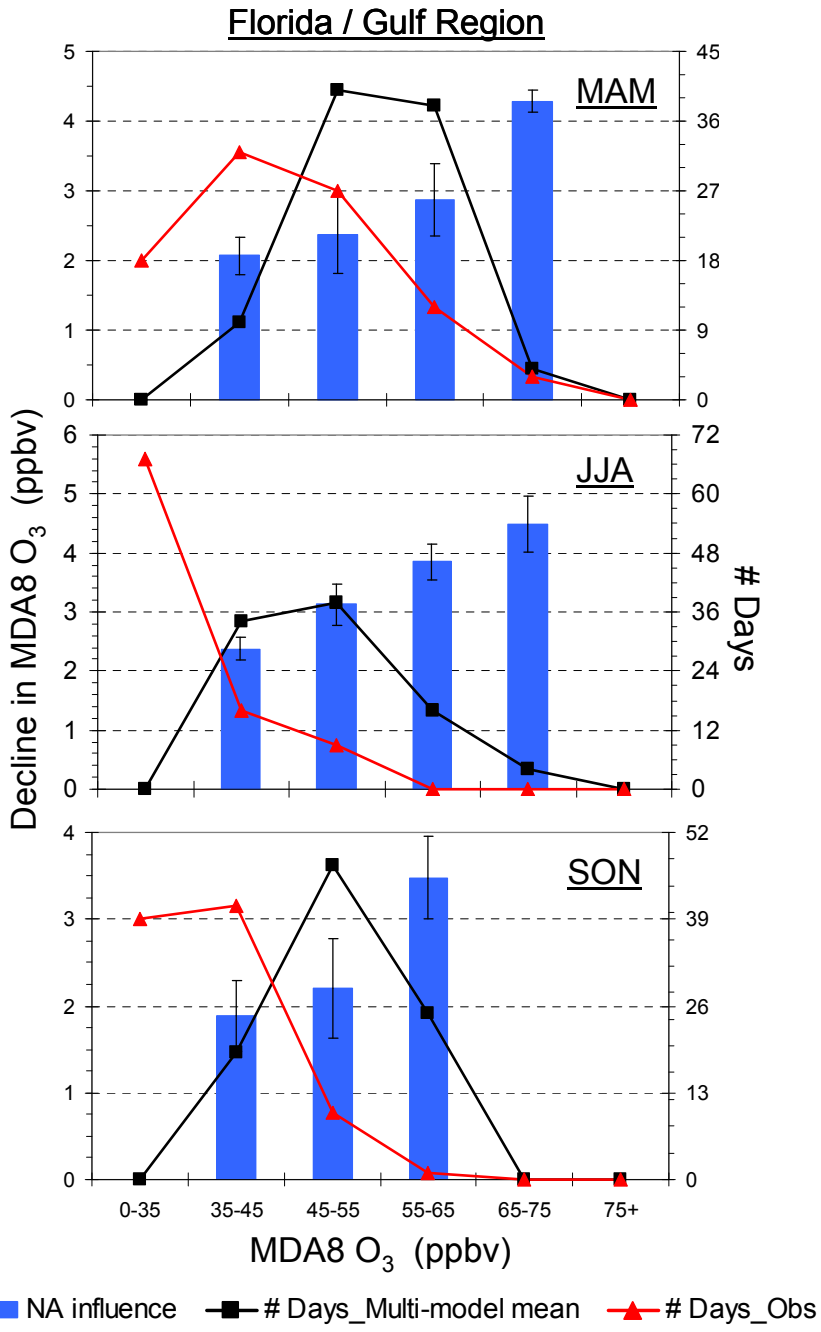


**Figure A9.** (cont'd)

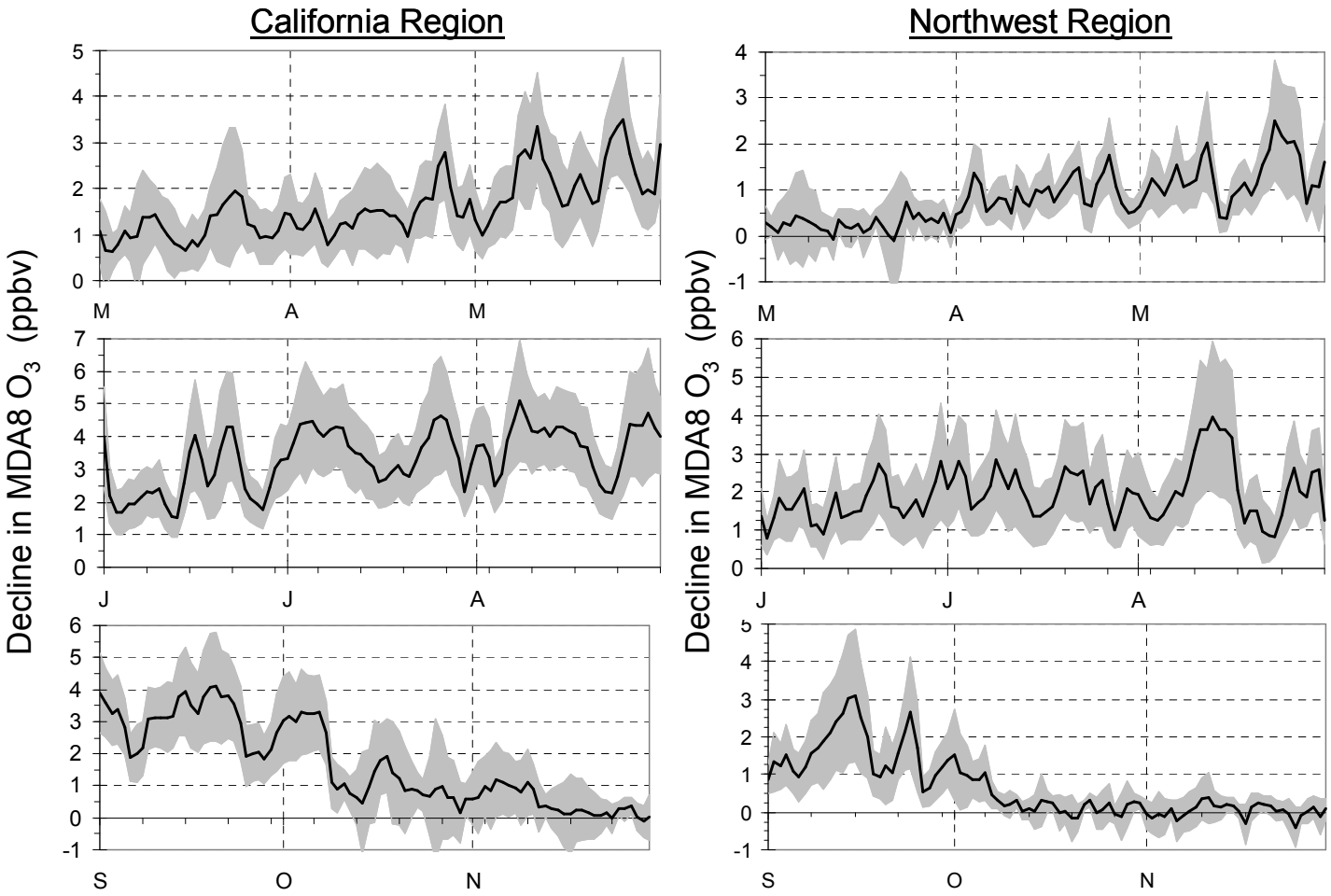


**Figure A10.** As in Fig. A8, but for a 20% emissions reduction of anthropogenic $O_3$-precursors ($NO_x$ + CO + NMVOC + aerosols) in the North American source region (shown in Fig. A3). Note the range of magnitudes on the y-axes.

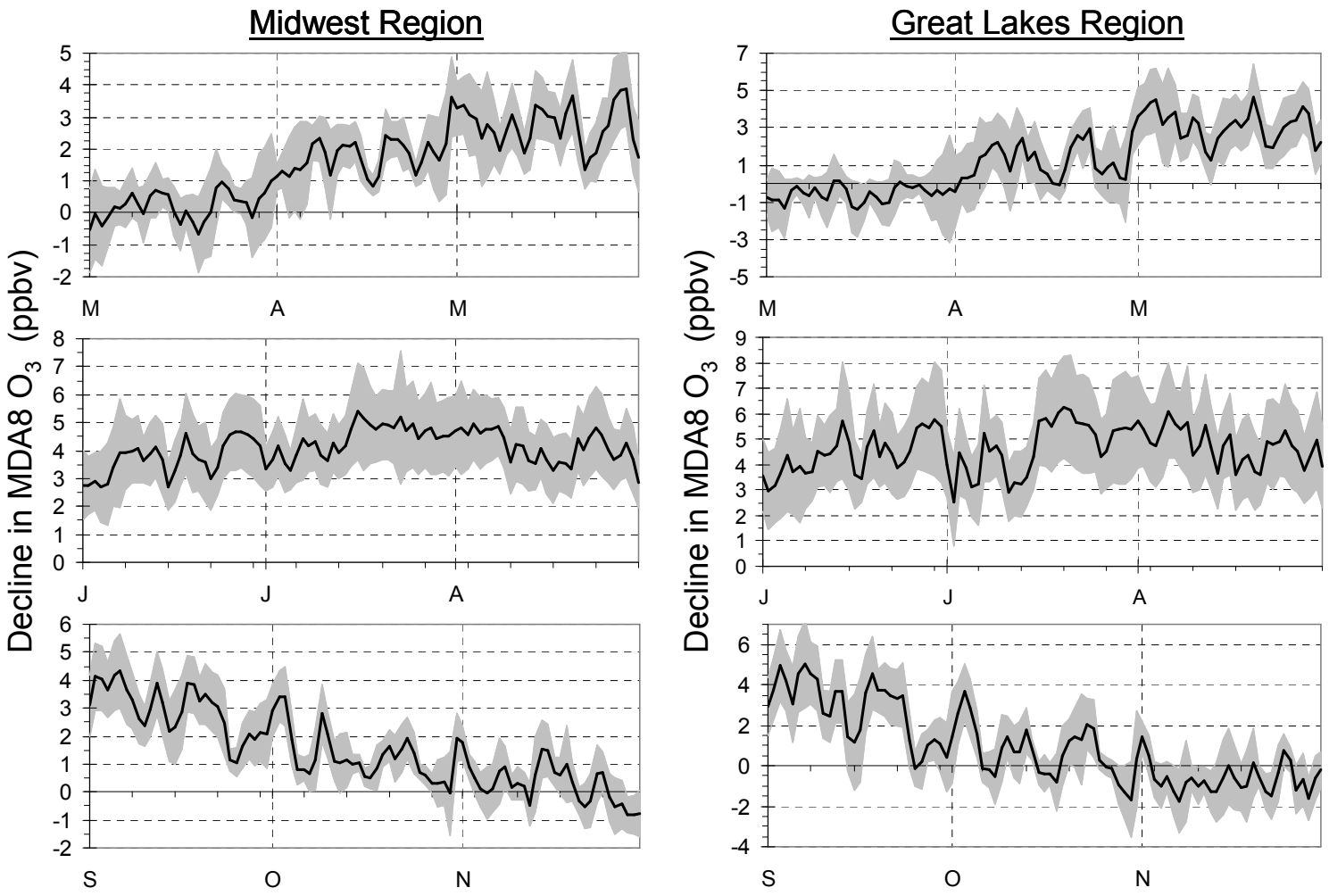


**Figure A10.** (cont'd)

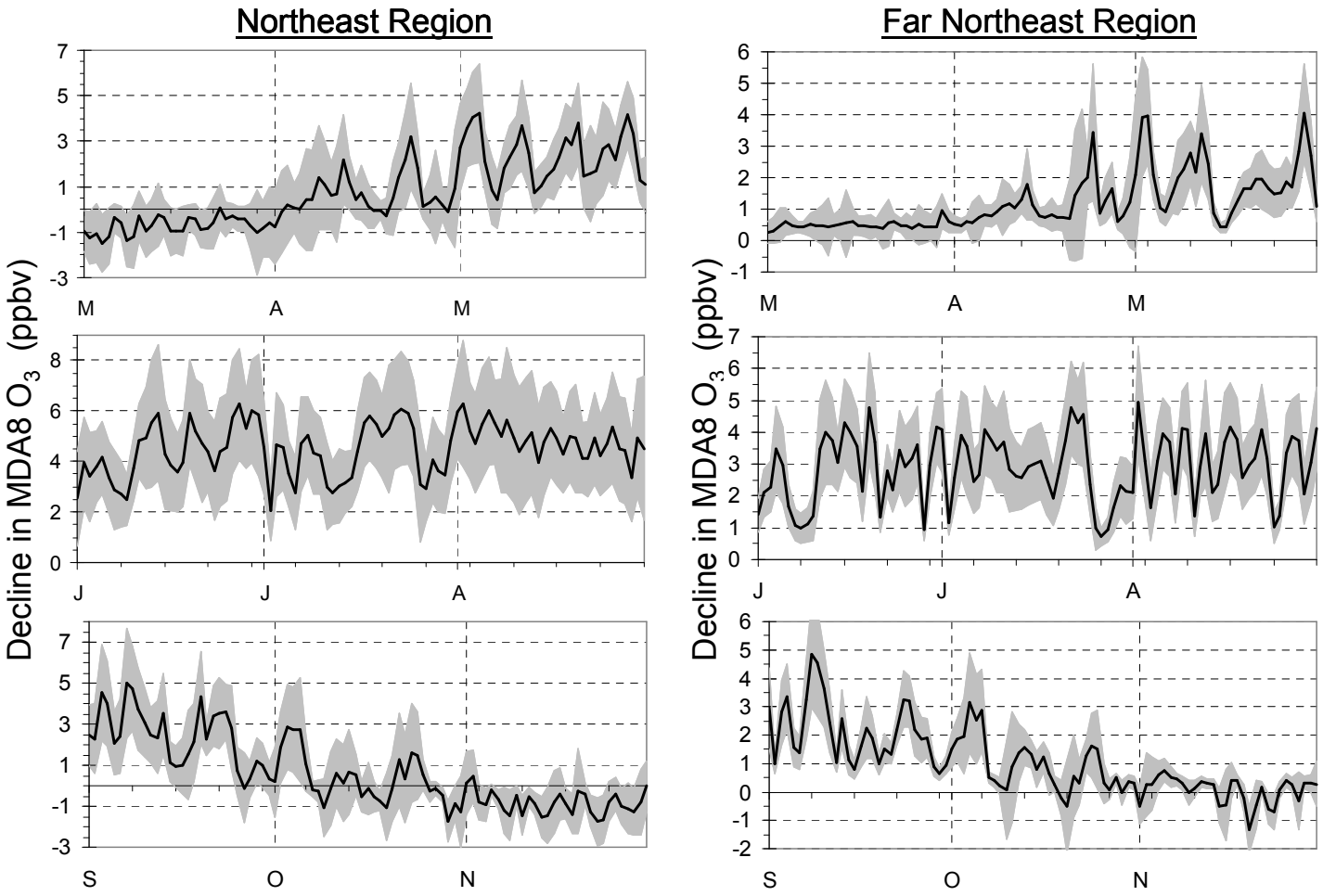


**Figure A10.** (cont'd)

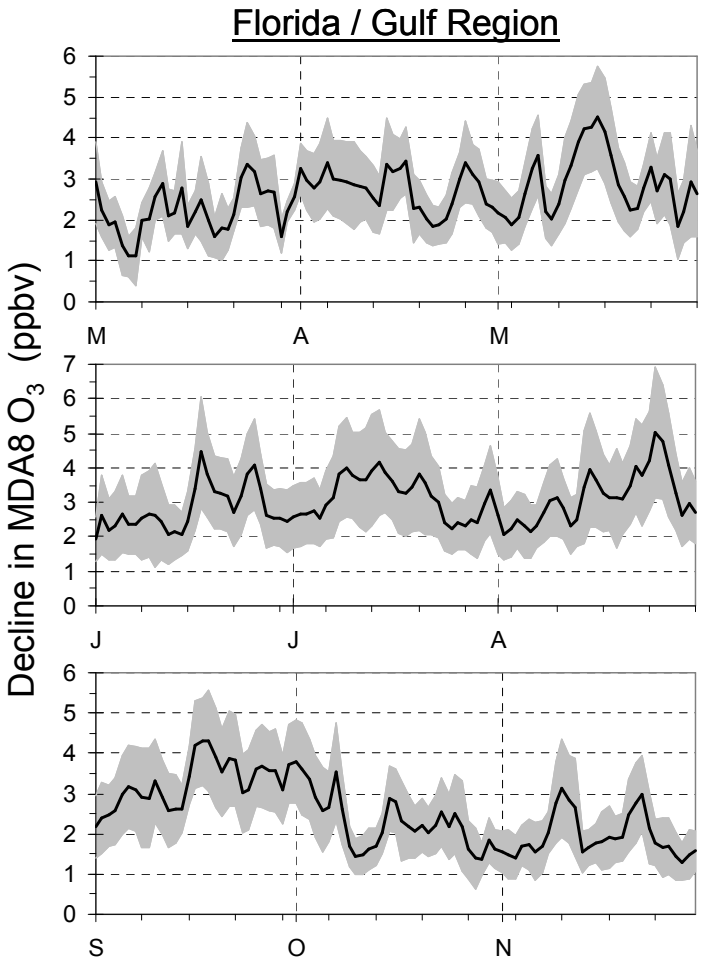


**Figure A10.** (cont'd)